



**HAL**  
open science

## Diammonium tetraborate dihydrate as hydrolytic by-product of ammonia borane in aqueous alkaline conditions

María-José Valero-Pedraza, Damien Alligier, Eddy Petit, Didier Cot, Dominique Granier, Karim Adil, Pascal Yot, Umit Demirci

### ► To cite this version:

María-José Valero-Pedraza, Damien Alligier, Eddy Petit, Didier Cot, Dominique Granier, et al.. Diammonium tetraborate dihydrate as hydrolytic by-product of ammonia borane in aqueous alkaline conditions. *International Journal of Hydrogen Energy*, 2020, 45 (16), pp.9927-9935. 10.1016/j.ijhydene.2020.01.223 . hal-02536900

**HAL Id: hal-02536900**

**<https://hal.science/hal-02536900>**

Submitted on 22 Aug 2022

**HAL** is a multi-disciplinary open access archive for the deposit and dissemination of scientific research documents, whether they are published or not. The documents may come from teaching and research institutions in France or abroad, or from public or private research centers.

L'archive ouverte pluridisciplinaire **HAL**, est destinée au dépôt et à la diffusion de documents scientifiques de niveau recherche, publiés ou non, émanant des établissements d'enseignement et de recherche français ou étrangers, des laboratoires publics ou privés.



Distributed under a Creative Commons Attribution - NonCommercial 4.0 International License

# Diammonium tetraborate dihydrate as hydrolytic by-product of ammonia borane in aqueous alkaline conditions

María-José VALERO-PEDRAZA<sup>1</sup>, Damien ALLIGIER<sup>1</sup>, Eddy PETIT<sup>1</sup>, Didier COT<sup>1</sup>, Dominique GRANIER<sup>2</sup>, Karim ADIL<sup>2</sup>, Pascal G. YOT<sup>2</sup>, Umit B. DEMIRCI<sup>1\*</sup>

<sup>1</sup> Institut Européen des Membranes, IEM – UMR 5635, Univ Montpellier, CNRS, ENSCM, Montpellier, France

<sup>2</sup> Institut Charles Gerhardt Montpellier, ICGM – UMR 5253, Univ Montpellier, CNRS, ENSCM, Montpellier, France

\* [umit.demirci@umontpellier.fr](mailto:umit.demirci@umontpellier.fr)

## Abstract

Ammonia borane  $\text{NH}_3\text{BH}_3$  is able to generate  $\text{H}_2$  by catalytic hydrolysis at ambient conditions. Such a potential has been much studied but the hydrolysis by-products, i.e. ammonium borates, have been little studied. As such we undertook a systematic work aiming at getting a sound understanding of the borates forming by hydrolysis. Contrary to what is commonly believed,  $\text{NH}_3\text{BH}_3$  (10 M) in aqueous alkaline (pH = 8) solution is not completely stable. Spontaneous hydrolysis takes place, resulting in the formation of by-products and precipitation of *borate crystals*. This means that long-term storage of concentrated AB solution is not possible. The *borate crystals* were analyzed with the help of various techniques and was identified as being diammonium tetraborate dihydrate  $(\text{NH}_4)_2\text{B}_4\text{O}_5(\text{OH})_4 \cdot 2\text{H}_2\text{O}$  (263.39 g mol<sup>-1</sup>). The crystal structure was solved and found to be monoclinic with a space group  $P2_1$ . The borate is an analog of borax  $\text{Na}_2\text{B}_4\text{O}_5(\text{OH})_4 \cdot 8\text{H}_2\text{O}$ . These results, among others, are reported in details hereafter and they are discussed in order to bring elements of response to the questions concerning storage of aqueous  $\text{NH}_3\text{BH}_3$  and recyclability of such a borate.

## Keywords

Ammonia borane; Borate; Hydrogen storage; Hydrolysis; Polyborate; Tetraborate.

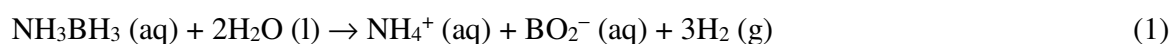
## 1. Introduction

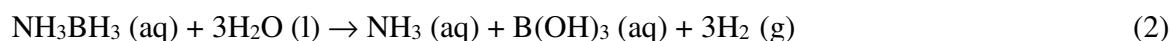
Ammonia borane  $\text{NH}_3\text{BH}_3$  (AB) is a prominent boron-based material in the field of chemical hydrogen storage. Though known since the middle of the last century [1], the interest in it, for the mentioned application, started in the mid-2010s, especially as a result of two pioneering works. On the one hand, Gutowska et al. [2] demonstrated that the dehydrogenation properties of AB under heating are substantially improved when a nanoscaffold (e.g. mesoporous silica) is used to destabilize it. On the other hand, Chandra and Xu [3] showed that rapid dehydrogenation of AB is feasible, at ambient conditions, by dissociation and catalytic hydrolysis. Since then, dehydrogenation of AB by thermolysis or hydrolysis has been widely investigated, each of these approaches having their own advantages and drawbacks [4-6].

Before AB, another boron-based material, namely sodium borohydride  $\text{NaBH}_4$ , showed interesting dehydrogenation properties by hydrolysis [7]. AB was suggested to be a good alternative mainly because  $\text{NaBH}_4$  is not stable in aqueous solution [8]. For example, Chandra and Xu [9] reported that a slightly concentrated (0.1 M) solution of AB (pH of 9.1) kept under argon atmosphere is fairly stable and, above all, much more stable than a  $\text{NaBH}_4$  solution. Hence, hydrolysis of AB requires a catalyst to generate  $\text{H}_2$  with fast kinetics [3], which has given rise to great efforts in developing a lot of active catalysts [10-13]. In contrast, other aspects related to the hydrolysis reaction (e.g. effective storage capacity maximization,  $\text{H}_2$  purity, reaction intermediates analysis, by-products identification) have been far less explored [5,6].

The basic argument against hydrolysis of  $\text{NaBH}_4$  is that sodium tetrahydroxyborate  $\text{NaB}(\text{OH})_4$ , the reaction by-product, is awkwardly transformed (i.e. reduced) back into  $\text{NaBH}_4$  [14]. Simply put, the B–O bond in the anion  $\text{B}(\text{OH})_4^-$  is, roughly, as stable as the C–O bond in  $\text{CO}_2$  [15], both compounds facing thus comparable conversion challenges. This also applies to AB in hydrolysis, and yet, little is known about its by-products.

Chandra and Xu [3,9] reported, without further discussion, the formation of boric acid  $\text{B}(\text{OH})_3$  and of the metaborate anion  $\text{BO}_2^-$ , as well as the formation of other borates that coexist in solution via pH-dependent equilibria:

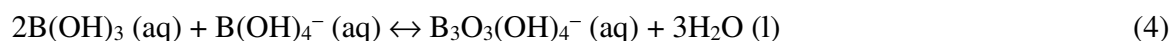




Mohajeri et al. [16] corroborated and, added that the by-product in solid state was crystallized  $\text{B}(\text{OH})_3$ . Using in situ  $^{11}\text{B}$  NMR, Liu et al. [17] concluded that the formation of aqueous  $\text{B}(\text{OH})_3$  (Eq. 2) took place, whereas Rachiero et al. [18,19], stressed on the formation of aqueous  $\text{B}(\text{OH})_4^-$ :



Both species, i.e.  $\text{B}(\text{OH})_3$  and  $\text{B}(\text{OH})_4^-$ , are likely to form and their formation is mainly pH-dependent (pKa of  $\text{B}(\text{OH})_3/\text{B}(\text{OH})_4^-$  equal to 9.1). Rachiero et al. [18,19] and Hannauer et al. [20] suggested reactions between the  $\text{B}(\text{OH})_3$  and  $\text{B}(\text{OH})_4^-$  entities, resulting in equilibria with polyborate species like  $\text{B}_3\text{O}_3(\text{OH})_4^-$ . The following path was notably suggested:



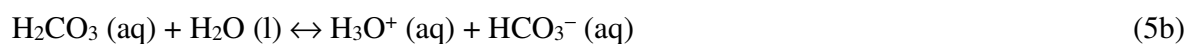
For the solid recovered after water extraction, they identified, by pattern matching, ammonium tetraborate tetrahydrate  $(\text{NH}_4)_2\text{B}_4\text{O}_7 \cdot 4\text{H}_2\text{O}$ . Ramachandran and Gagare [21] studied a concentrated AB solution (10.8 M). A crystallized borate salt was recovered and, by X-ray crystallography, its structure was determined, at 50% probability, as ammonium tetraborate hydrate  $(\text{NH}_4)_2\text{B}_4\text{O}_5(\text{OH})_4 \cdot 1.4\text{H}_2\text{O}$ . Moussa et al. [22] prepared a set of borates by extraction of water at different temperatures ( $-50$ ,  $0$ ,  $80$ ,  $120$ ,  $200$  and  $300^\circ\text{C}$ ). A series of ammonium pentaborates (e.g.  $\text{NH}_4\text{B}_5\text{O}_6(\text{OH})_4 \cdot 2\text{H}_2\text{O}$  and  $\text{NH}_4\text{B}_5\text{O}_6(\text{OH})_4$ ) were suggested together with  $\text{B}(\text{OH})_3$ ,  $\text{HBO}_2$  and  $\text{B}_2\text{O}_3$  (depending on the temperature). Chou et al. [23] focused on incomplete hydrolysis of AB, which was performed by using a limited amount of water (less than the stoichiometry in Eq. 3). Mixtures of  $\text{B}(\text{OH})_3$  and metaboric acid  $\text{HBO}_2$  were found to be the dominant products in such conditions.

It is important to have a sound understanding of the borates forming by hydrolysis of AB. Borates form, but their nature depends on a number of experimental factors (AB concentration, solution pH, water amount, atmosphere, water extraction and drying processes). On another note, AB is not so stable in aqueous alkaline solution. For example, a careful analysis of the  $^{11}\text{B}$  NMR data reported by Chandra and Xu [3,9] shows at least one additional signal at a positive chemical shifts, which was due to a borate species. Hence, we initiated a new study aiming at recovering and analyzing crystallized borates forming by spontaneous hydrolysis of AB (10 M). We isolated

crystals of diammonium tetraborate dihydrate  $(\text{NH}_4)_2\text{B}_4\text{O}_5(\text{OH})_4 \cdot 2\text{H}_2\text{O}$  ( $263.39 \text{ g mol}^{-1}$ ). This compound is a less-hydrated ammonium analog of borax  $\text{Na}_2\text{B}_4\text{O}_5(\text{OH})_4 \cdot 8\text{H}_2\text{O}$  (disodium tetraborate octahydrate). Our results are described hereafter and discussed to bring elements of response to the questions concerning storage of AB in aqueous solution.

## 2. Experimental

Ammonia borane  $\text{NH}_3\text{BH}_3$  (borane-ammonia complex; CAS number 13774-81-7; 97% from Merck) was stored in an argon-filled glove box (MBraun M200B;  $\text{O}_2$  and  $\text{H}_2\text{O} < 0.1 \text{ ppm}$ ). Sodium hydroxide  $\text{NaOH}$  (CAS number 1310-73-2; from Alfa Aesar) was also used as received. With respect to deionized ultra-pure water (Milli-Q grade, resistivity  $> 18 \text{ M}\Omega \text{ cm}$ ), it was systematically bubbled with argon just after extraction from our purification system, and it was used to prepare an alkaline solution (pH adjusted at 8) under argon flux. All of the solutions were in fact kept under argon atmosphere to avoid dissolution of carbon dioxide  $\text{CO}_2$  from air and subsequent formation of carbonic acid  $\text{H}_2\text{CO}_3$ :



The  $\text{NH}_3\text{BH}_3$  solution (10 M) was prepared as follows. In the glove box, 308 mg of  $\text{NH}_3\text{BH}_3$  was weighted and transferred in a vial which was sealed with a septum. Under argon, 1 mL of the aqueous alkaline solution was injected through the septum. After complete dissolution of  $\text{NH}_3\text{BH}_3$ , the sealed vial, under an argon atmosphere, was put in a heat chamber initially at  $35 \text{ }^\circ\text{C}$  (dark conditions). The temperature of the chamber was decreased by  $1 \text{ }^\circ\text{C}$  every week. Degassing (to evacuate the generated  $\text{H}_2$ ) was performed when the septum got curved, which was done by briefly puncturing the septum. Crystals were visible when the temperature dropped below  $25 \text{ }^\circ\text{C}$ . They were extracted from the solution and transferred in a clean vial (in the glove box). They were put under vacuum overnight and finally stored under argon atmosphere.

The crystals were visualized using a digital microscope (Keyence VHX-6000) and, analyzed by different techniques: Fourier transform infrared (FTIR) spectroscopy (FTIR; IS50 Thermo Fisher Scientific); Raman spectroscopy (Horiba Jobin Yvon LabRAM 1B; laser Ar/Kr 100 mW 647.1

nm); X-ray photoelectron spectroscopy (XPS; ESCALAB 250 from Thermo Electron; monochromatic source Al K $\alpha$  ray 1486.6 eV; analyzed surface of 400  $\mu$ m diameter; binding energies (BE) of all core levels referred to the C–C of C1s carbon at 284.8 eV); thermogravimetric (TG) analysis (Netzsch STA 449 F1 Jupiter) coupled to mass spectrometry (MS; Netzsch QMS 403D Aëolos Quadro) for gas analysis; and, differential scanning calorimetry (DSC; DSC; Q600, TA Instruments).  $^{11}\text{B}$  nuclear magnetic resonance (NMR) spectroscopy (Bruker AVANCE-300; probe head BBO10, 96.29 MHz, D $_2$ O in a capillary tube) was used to analyze the solutions obtained by dissolution of the crystals in deionized water and methanol (CAS number 67-56-1;  $\geq 99.9\%$  from Merck).

Part of the as-obtained single crystal was analyzed by X-ray diffraction. X-ray single-crystal structural data were collected on a Bruker D8 VENTURE equipped with a PHOTON II CPAD detector and a microfocus X-ray source with Cu-K $\alpha$  radiation ( $\lambda = 1.54184 \text{ \AA}$ ) operating at 50 kV and 1 mA. A suitable crystal was chosen and mounted on a 150  $\mu$ m aperture Dual-Thickness Microloop. The data collection was performed at  $-173 \text{ }^\circ\text{C}$  and at ambient temperature. The as-obtained unit cell and space group showed that the structures were identical. We therefore decided to report the data collected at  $-173 \text{ }^\circ\text{C}$ . The single crystal X-ray diffraction allowed collecting a total of 1496 frames. The total exposure time was 8.31 h. The frames were integrated with the Bruker SAINT Software package using a narrow-frame algorithm. The integration of the data using a monoclinic unit cell yielded a total of 4196 reflections to a maximum  $\theta$  angle of  $55.06^\circ$  (resolution of  $0.94 \text{ \AA}$ ). The final cell constants (as reported hereafter, in sub-section 3.4) are based upon the refinement of the XYZ-centroids of 3948 reflections above  $20 \sigma(I)$  with  $12.38^\circ < 2\theta < 110.1^\circ$ . The data were corrected for absorption effects using the Multi-Scan method (SADABS). The ratio of minimum to maximum apparent transmission was 0.797. The space group was determined using XPREP implemented in APEX3. The structure was solved using SHELXS-97 (direct methods) and refined using SHELXL-2014 (full-matrix least-squares on  $F^2$ ) contained in WinGX. The crystal data, refinement conditions and crystal structure are reported hereafter, in sub-section 3.4.

### 3. Results

#### 3.1. Preliminary observation

Crystallization (and precipitation) of pure AB generally results in needle-like forms [24]. In our conditions, bulky and shaped crystals were recovered. An example is shown in Figure 1. The crystal looks very similar to crystals of ammonium pentaborate  $(\text{NH}_4)_2\text{O}\cdot 5\text{B}_2\text{O}_3\cdot 8\text{H}_2\text{O}$  [25]. From this observation, evolution of AB into a borate, by hydrolysis, was assumed to take place. Hereafter, the as-formed solid will be called *borate crystal*.



**Figure 1.** Digital microscope observation of one of our millimeter-scale *borate crystals* recovered after hydrolysis of AB in alkaline conditions: magnification  $\times 100$ ; angle of rotation  $0^\circ$ ; scale bar  $100\ \mu\text{m}$ .

#### 3.2. Analysis by spectroscopy

The formation of a borate was first verified by  $^{11}\text{B}$  NMR spectroscopy. Fragments of the *borate crystal* were solubilized in two different solvents, namely water and methanol (Figure 2). With the former solvent, a singlet peaking at  $+16.2\ \text{ppm}$  is noticed; it is typical of a borate [26]. With methanol as solvent, there are two overlapping singlets peaking at  $+18.8$  and  $+17\ \text{ppm}$ . It is likely that some  $-\text{OH}$  groups of the borate were substituted by  $-\text{OCH}_3$  groups.

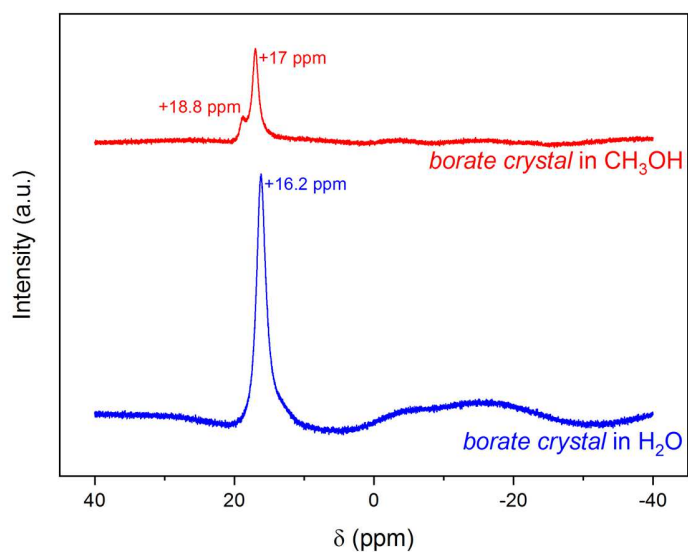


**Figure 2.**  $^{11}\text{B}$  NMR spectra of the *borate crystal* in water and in methanol.

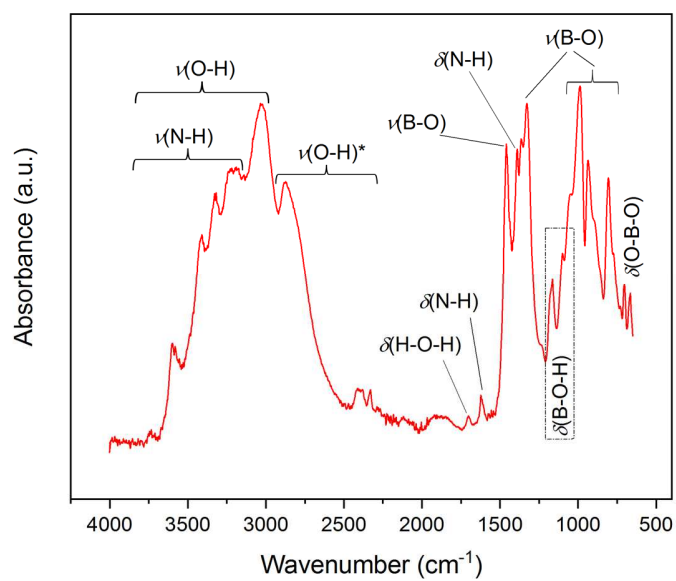


**Figure 3.** FTIR spectrum of the *borate crystal* (\* for O–H bonds involved in hydrogen bonding).



The FTIR fingerprint of the *borate crystal* (Figure 3) is comparable to that of di-, tetra- and penta-borates [27]. Stretching and deformation modes for B–O, O–H (including O–H involved in hydrogen bonding), B–O–H, and N–H bonds can be seen. They confirm the transformation of AB into a borate species.

Similar observations can be made for the Raman spectrum (Figure 4). Otherwise, there is an intense band at  $583\text{ cm}^{-1}$  due to B–O bonds. Interestingly, it matches the band due to B–O bonds found in the anion  $\text{B}_4\text{O}_5(\text{OH})_4^{2-}$  [28,29], and specifically in borax  $\text{Na}_2\text{B}_4\text{O}_5(\text{OH})_4 \cdot 8\text{H}_2\text{O}$  [30].

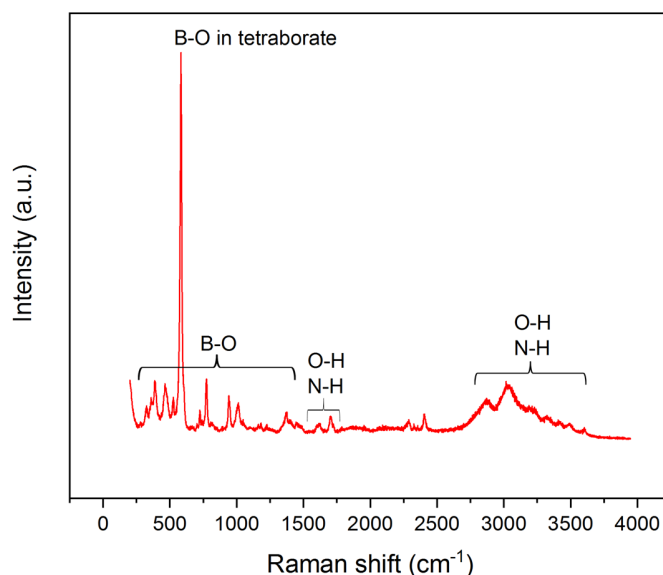


**Figure 4.** Raman spectrum of the *borate crystal*.

The *borate crystal* was analyzed by XPS (Figure 5). Besides the C element, the survey scan shows the presence of B, N and O. The binding energy of B (1s) is 192.7 eV, which is typical of a boron oxide. According to the NIST database [31], the energy 192.7 eV ( $\pm 0.1$  eV) is typical of e.g. boric acid  $\text{B}(\text{OH})_3$ , boron oxide  $\text{B}_2\text{O}_3$ , the tetraborate anion  $\text{B}_4\text{O}_7^{2-}$ , ammonium tetraborate tetrahydrate  $(\text{NH}_4)_2\text{B}_4\text{O}_7 \cdot 4\text{H}_2\text{O}$ , and also  $(\text{NH}_4)_2\text{O} \cdot 5\text{B}_2\text{O}_3 \cdot 8\text{H}_2\text{O}$ . The binding energy of O (1s) is 532.5 eV and is comparable to that of e.g.  $\text{B}_2\text{O}_3$ . The binding energy of N (1s) is 401.9 eV, a

value found for a number of ammonium salts. It may be concluded that the XPS data suggest the formation of an ammonium (poly)borate.

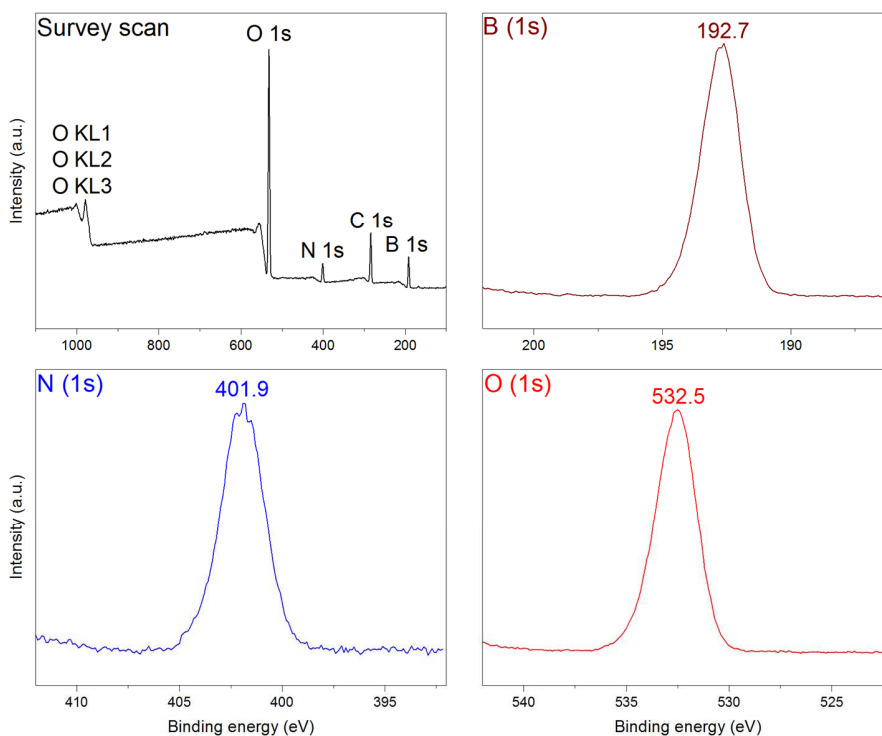


**Figure 5.** XPS spectra of the *borate crystal*: i.e. survey scan, and focuses on B (1s), N (1s) and O (1s).

### 3.3. Thermal and calorimetric analysis

The thermal behavior of the *borate crystal* was studied by TG analysis and DSC (Figure 6). The released gases were analyzed by MS (Figure 6) and the following  $m/z$  values were collected (in order of the signals intensity): 17, 18, 16 and 15. The intensity of the signal  $m/z = 18$  is comparable to that of the signal  $m/z = 17$ . For pure  $\text{H}_2\text{O}$ , the relative intensity between these two signals should have been 5:1. In our conditions, the relative intensity is close to 1. Our results thus indicate that  $\text{H}_2\text{O}$  (with  $m/z = 18, 17$  and 16) formed by dehydration and  $\text{NH}_3$  (with  $m/z = 17, 16$  and 15) formed by deammoniation. Similar observations are reported elsewhere, for the thermal decomposition of  $(\text{NH}_4)_2\text{O} \cdot 5\text{B}_2\text{O}_3 \cdot 8\text{H}_2\text{O}$  [25].

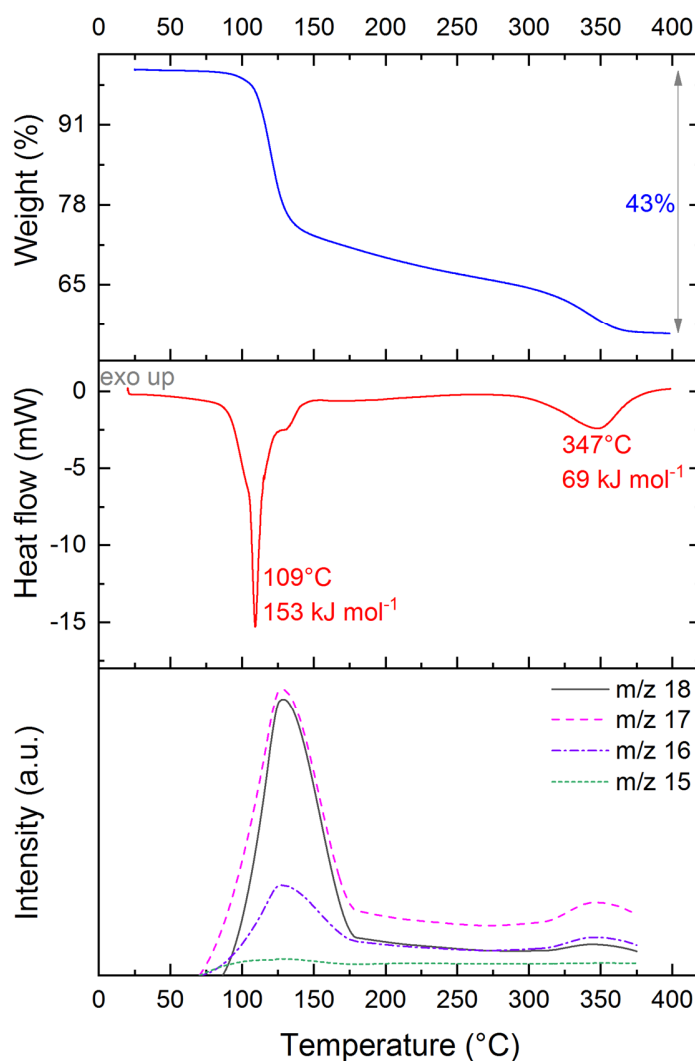


**Figure 6.** TG analysis, DSC and MS results for the *borate crystal* (heating rate  $5\text{ }^{\circ}\text{C min}^{-1}$ ).

The thermal decomposition of the *borate crystal* is stepwise, showing two main weight losses. From 75 to 250  $^{\circ}\text{C}$ , the *borate crystal* overcomes a significant loss of  $\text{H}_2\text{O}$  and  $\text{NH}_3$  (33.2% in weight); the process is featured by an endothermic signal ( $153\text{ kJ mol}^{-1}$ ) peaking at 109  $^{\circ}\text{C}$ . A roughly comparable energy ( $187\text{ kJ mol}^{-1}$ ) was reported for dehydration (3  $\text{H}_2\text{O}$  out of 8) of  $(\text{NH}_4)_2\text{O}\cdot 5\text{B}_2\text{O}_3\cdot 8\text{H}_2\text{O}$ , the process peaking at higher temperature (175  $^{\circ}\text{C}$ ) [25]. Above 250  $^{\circ}\text{C}$  and up to 400  $^{\circ}\text{C}$ , the *borate crystal* continues to decompose. The weight loss is less important (9.8%). This event is featured by an endothermic signal ( $69\text{ kJ mol}^{-1}$ ) peaking at 347  $^{\circ}\text{C}$ . A

similar energy ( $67 \text{ kJ mol}^{-1}$ ) was reported for  $(\text{NH}_4)_2\text{O}\cdot 5\text{B}_2\text{O}_3\cdot 5\text{H}_2\text{O}$ ; this polyborate liberated 2 equiv  $\text{H}_2\text{O}$  in a process peaking at  $311 \text{ }^\circ\text{C}$  [25].

Our TG and DSC curves were compared to curves obtained with a compound reported to be ammonium tetraborate tetrahydrate ( $263.2 \text{ g mol}^{-1}$ ) [32]. Unfortunately, there is no detail about its preparation or origins. From the information that can be found on the internet (especially from suppliers of chemicals), this compound would be  $(\text{NH}_4)_2\text{B}_4\text{O}_7\cdot 4\text{H}_2\text{O}$  (Figure 7). The comparison shows similarities (Table 1): above  $75 \text{ }^\circ\text{C}$  the TG results are similar; the endothermic signals peak at similar temperatures; there is the co-release of  $\text{H}_2\text{O}$  and  $\text{NH}_3$  over the range  $75\text{-}400 \text{ }^\circ\text{C}$ . The comparison also shows one key difference: with  $(\text{NH}_4)_2\text{B}_4\text{O}_7\cdot 4\text{H}_2\text{O}$ , there is a preliminary weight loss, below  $75 \text{ }^\circ\text{C}$ , due to the release of 1 equiv  $\text{H}_2\text{O}$  (release of crystal water), which is associated to an endothermic signal peaking at  $59 \text{ }^\circ\text{C}$ . In terms of weight loss measured at  $400 \text{ }^\circ\text{C}$ , the values are roughly comparable: the loss is 43% for the present borate and it is 40.2% for  $(\text{NH}_4)_2\text{B}_4\text{O}_7\cdot 4\text{H}_2\text{O}$  (if the dehydration process occurring below  $75 \text{ }^\circ\text{C}$  is not taken into account). From these observations, it is reasonable to conclude that the borate reported herein and the  $(\text{NH}_4)_2\text{B}_4\text{O}_7\cdot 4\text{H}_2\text{O}$  reported elsewhere looks similar, even though our borate has structure water only.

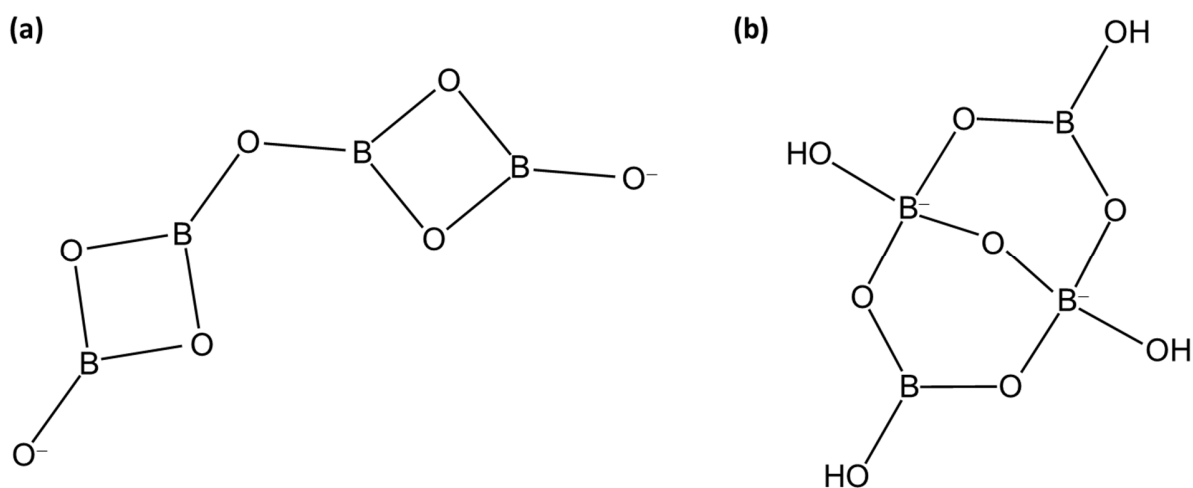


**Table 1.** Comparison of the present *borate crystal* to  $(\text{NH}_4)_2\text{B}_4\text{O}_7 \cdot 4\text{H}_2\text{O}$  in reference [32], in terms of TG analysis, DSC and MS results.

Temperature range (°C)		The <i>borate crystal</i> <i>present work</i>	$(\text{NH}_4)_2\text{B}_4\text{O}_7 \cdot 4\text{H}_2\text{O}$ <i>in ref. [32]</i>
20-75	Weight loss (%) by TG analysis	0	6.9
	DSC peak temperature (°C)		59
	Evolving gases by MS		H <sub>2</sub> O
75-250	Weight loss (%) by TG analysis	33.2	28.2
	DSC peak temperature (°C)	109	110
	Evolving gases by MS	H <sub>2</sub> O and NH <sub>3</sub>	H <sub>2</sub> O and NH <sub>3</sub>
251-400	Weight loss (%) by TG analysis	9.8	12
	DSC peak temperature (°C)	347	335
	Evolving gases by MS	H <sub>2</sub> O and NH <sub>3</sub>	H <sub>2</sub> O and NH <sub>3</sub>
20-400	Weight loss by TG analysis	43	47.1

### 3.4. Structural analysis

A portion of the *borate crystal* was analyzed by single crystal X-ray diffraction. The crystal data and the refinement conditions are shown in Table 2. In good agreement with the results reported above, the *borate crystal* was identified to be an ammonium polyborate salt of formulae  $(\text{NH}_4)_2\text{B}_4\text{O}_5(\text{OH})_4 \cdot 2\text{H}_2\text{O}$  (diammonium tetraborate dihydrate; 263.39 g mol<sup>-1</sup>). The crystal system is monoclinic, and the space group is  $P2_1$ . The cell constants were found to be such as:  $a = 7.15996(6)$  Å,  $b = 10.6344(9)$  Å,  $c = 7.2331(6)$  Å,  $\beta = 98.593(3)^\circ$ ,  $V = 544.55(5)$  Å<sup>3</sup>. The crystal structure is shown in Figure 8.

Diammonium tetraborate dihydrate is structured around the anion  $\text{B}_4\text{O}_5(\text{OH})_4^{2-}$  (Figure 9), as is the case for borax [33]. They both crystallize in monoclinic system, but they have different space groups ( $P2_1$  and  $C2/c$  respectively). Diammonium tetraborate dihydrate is comparable to the compound reported by Ramachandran and Gagare [21]. They suggested the formulae  $(\text{NH}_4)_2\text{B}_4\text{O}_5(\text{OH})_4 \cdot 1.4\text{H}_2\text{O}$ , which was crystallographically determined at 50% probability. Our  $(\text{NH}_4)_2\text{B}_4\text{O}_5(\text{OH})_4 \cdot 2\text{H}_2\text{O}$  and the  $(\text{NH}_4)_2\text{B}_4\text{O}_5(\text{OH})_4 \cdot 1.4\text{H}_2\text{O}$  are isostructural (monoclinic, s.g.  $P2_1$ ). The cell constants of  $(\text{NH}_4)_2\text{B}_4\text{O}_5(\text{OH})_4 \cdot 1.4\text{H}_2\text{O}$  were calculated as being as follows:  $a = 7.1997(8)$  Å,  $b = 10.6039(6)$  Å,  $c = 7.2604(8)$  Å,  $\beta = 98.537(6)^\circ$ ,  $V = 548.153$  Å<sup>3</sup>.

**Table 2.** Space group, unit cell parameters, goodness of fit (GoF), R values, and structural parameters for the refined structure of the *borate crystal* identified to be  $(\text{NH}_4)_2\text{B}_4\text{O}_5(\text{OH})_4 \cdot 2\text{H}_2\text{O}$ .

Empirical formula	$(\text{NH}_4)_2\text{B}_4\text{O}_5(\text{OH})_4 \cdot 2\text{H}_2\text{O}$ $\text{B}_4\text{H}_{16}\text{N}_2\text{O}_{11}$	
Formula weight ( $\text{g mol}^{-1}$ )	263.39	
Temperature ( $^\circ\text{C}$ )	-173	
Wavelength ( $\text{\AA}$ )	1.54178	
Crystal system, space group	Monoclinic, $P2_1$	
Unit cell dimensions	$a$ ( $\text{\AA}$ )	7.15996(6)
	$b$ ( $\text{\AA}$ )	10.6344(9)
	$c$ ( $\text{\AA}$ )	7.2331(6)
	$\beta$ ( $^\circ$ )	98.593(3)
Cell volume ( $\text{\AA}^3$ )	544.55(8)	
$Z$	2	
Calculated density ( $\text{g cm}^{-3}$ )	1.606	
Absorption coefficient ( $\text{mm}^{-1}$ )	1.42	
$F(000)$	276	
Crystal size (mm)	$0.02 \times 0.03 \times 0.03$	
$\theta$ range for data collection ( $^\circ$ )	6.2–68.3	
Limiting indices	$-8 \leq h \leq 8, -12 \leq k \leq 12, -8 \leq l \leq 8$	
Completeness to $\theta = 68.3^\circ$	99.7%	
Refinement method	Full-matrix least-squares on $F^2$	
Data / restraints / parameters	1989 / 14 / 191	
Goodness-of-fit on $F^2$	1.14	
Final $R$ indices [ $I > 2\sigma(I)$ ]	0.036 and 0.039	
$R$ indices (all data)	0105 and 0.114	
Largest diff. peak and hole ( $\text{e \AA}^{-3}$ )	0.50 and -0.56	

## 4. Discussion

In our conditions, the concentrated solution of AB (10 M) evolved towards formation and precipitation of diammonium tetraborate dihydrate  $(\text{NH}_4)_2\text{B}_4\text{O}_5(\text{OH})_4 \cdot 2\text{H}_2\text{O}$ . For diluted solutions of AB, the main products are generally  $\text{B}(\text{OH})_3$  and  $\text{B}(\text{OH})_4^-$ . Depending on the experimental conditions, especially the pH, these two species were suggested to coexist [3,9,16] or preferentially form (the one at the expense of the other) [17-19]. Nevertheless, some

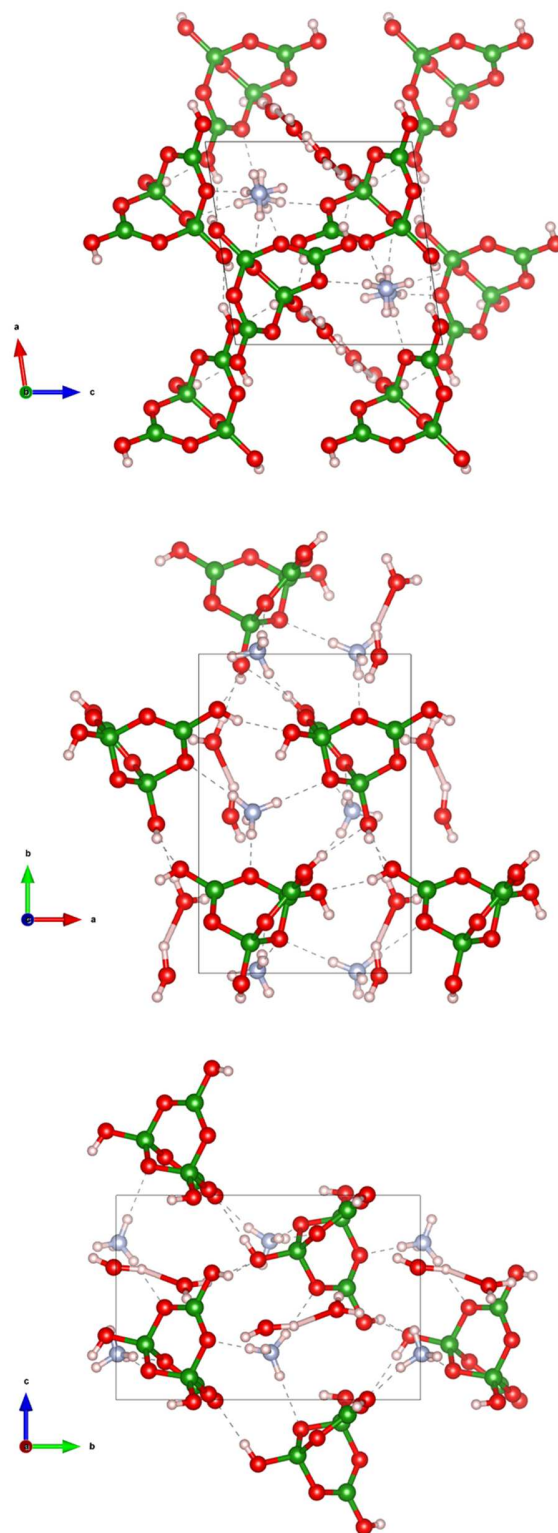
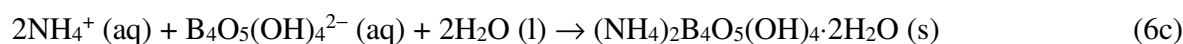
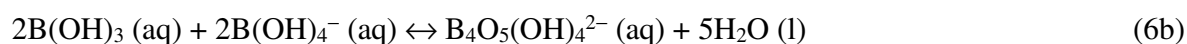
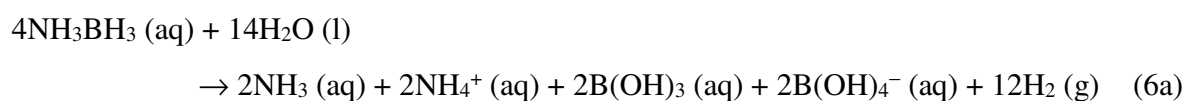


**Figure 8.** Crystal structure of the *borate crystal*  $(\text{NH}_4)_2\text{B}_4\text{O}_5(\text{OH})_4 \cdot 2\text{H}_2\text{O}$  along the a, b and c crystallographic axes. The pink, green, red and blue spheres correspond to the H, B, O and N atoms respectively.

form of consensus exists on the fact that, after the hydrolysis reaction,  $B(OH)_3$  and  $B(OH)_4^-$  interact, polyborates form, and equilibria between all of these species take place [3,9,16-19,22]. In fact, this is a well-documented property of  $B(OH)_3$  and  $B(OH)_4^-$ . For instance, Spessard [34] and Mesmer et al. [35] in the 1970s, and more recently Zhou et al. [36], investigated such equilibria in different conditions (pH, in the presence of neutral salt, at elevated temperature). It was established that there is an equilibrium leading to the anion  $B_4O_5(OH)_4^{2-}$  (Eq. 6b), which may explain the precipitation of  $(NH_4)_2B_4O_5(OH)_4 \cdot 2H_2O$  in our experimental conditions:



The balanced chemical equation is then:

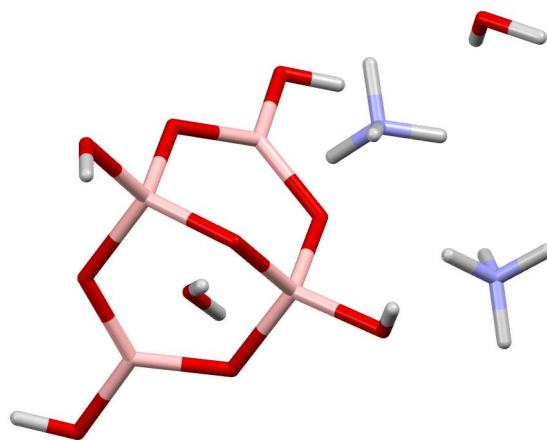


**Figure 9.** The  $B_4O_5(OH)_4^{2-}$  anion of the diammonium tetraborate dihydrate, consistently with the molecular structure shown in Figure 7b. The  $NH_4^+$  cations and the two  $H_2O$  molecules are also shown.

It is of interest to discuss the two “free”  $NH_3$  molecules shown in Eq. 6d. They can pass in the gas phase, being then liberated together with  $H_2$  generated by hydrolysis, as reported elsewhere [17,21,37]. This causes problems. The first one is related to the pollution of the  $H_2$  stream [38]. Purification is then required which is detrimental to the cost of the technology. The second problem can be discussed in terms of “green chemistry” [39]. Loss of the aforementioned  $NH_3$



molecules runs counter to the “green chemistry” principles like the following ones: “prevent waste”, “maximize atom economy”, “design chemicals and products to degrade after use”.

As briefly mentioned in the introduction, sodium borohydride in hydrolytic conditions has been criticized because of its instability in water at any pH [8]. AB was then presented as a stable alternative and it has been widely investigated. However, AB also evolves, spontaneously, in aqueous alkaline solution (i.e. in the absence of a catalyst). In our conditions, the AB concentration is high (10 M), which is realistic from the point of the view of a possible technological application. In such conditions, crystals of  $(\text{NH}_4)_2\text{B}_4\text{O}_5(\text{OH})_4 \cdot 2\text{H}_2\text{O}$  precipitate after some days. In other words, AB in hydrolytic conditions should encounter the same problems as sodium borohydride [40], namely, difficult long-term storage of concentrated AB solutions because of evolution by hydrolysis, safety issues because of uncontrolled generation of  $\text{H}_2$ , and plugging of storage system pipes due to precipitation of borate crystals.

Little efforts have been focused on the identification of the condition-dependent borate products and, in conjunction with this, on the development of AB-dedicated recycling and regeneration approaches [5,6]. Here, we have shown the precipitation of  $(\text{NH}_4)_2\text{B}_4\text{O}_5(\text{OH})_4 \cdot 2\text{H}_2\text{O}$ . It is an analog of borax  $\text{Na}_2\text{B}_4\text{O}_5(\text{OH})_4 \cdot 2\text{H}_2\text{O}$ . Borax is the boron source in the process leading to the production of  $\text{NaBH}_4$  via the so-called Brown-Schlesinger process: i.e. acidic attack ( $\text{H}_2\text{SO}_4$ ) of  $\text{Na}_2\text{B}_4\text{O}_5(\text{OH})_4 \cdot 2\text{H}_2\text{O}$  to form  $\text{B}(\text{OH})_3$ ; reaction of  $\text{B}(\text{OH})_3$  with methanol resulting in  $\text{B}(\text{OCH}_3)_3$ ; and, reduction of  $\text{B}(\text{OCH}_3)_3$  by  $\text{NaH}$  to get  $\text{NaBH}_4$  [41]. The present  $(\text{NH}_4)_2\text{B}_4\text{O}_5(\text{OH})_4 \cdot 2\text{H}_2\text{O}$  could be directly used to be transformed into  $\text{NaBH}_4$  by slightly adapting the aforementioned process. Otherwise, the NMR results presented above have shown transformation of  $(\text{NH}_4)_2\text{B}_4\text{O}_5(\text{OH})_4 \cdot 2\text{H}_2\text{O}$  by reaction with methanol. One may assume that  $\text{B}(\text{OCH}_3)_3$  formed. Further works are required to clear up this point; for instance, such  $\text{B}(\text{OCH}_3)_3$  might be the key compound of a modified version of the aforementioned Brown-Schlesinger process.

## 5. Conclusion

In the present work, we considered an aqueous alkaline solution of concentrated AB (10 M). Spontaneous hydrolysis of AB took place, resulting in generation of H<sub>2</sub> and, formation and precipitation of *borate crystals*. Aqueous AB is thus not stable, in our conditions, and long-term storage of such a fuel appears to be difficult. The *borate crystals* were isolated to be analyzed by various techniques, and the collected data indicated the formation of diammonium tetraborate dihydrate (NH<sub>4</sub>)<sub>2</sub>B<sub>4</sub>O<sub>5</sub>(OH)<sub>4</sub>·2H<sub>2</sub>O (263.39 g mol<sup>-1</sup>), an ammonium analog of borax Na<sub>2</sub>B<sub>4</sub>O<sub>5</sub>(OH)<sub>4</sub>·8H<sub>2</sub>O. The crystal structure was solved and was found to be as follows: monoclinic, space group *P2*<sub>1</sub>, *Z* = 2, *a* = 7.15996(6) Å, *b* = 10.6344(9) Å, *c* = 7.2331(6) Å, *β* = 98.704(3) °, *V* = 544.5(5) Å<sup>3</sup>. Diammonium tetraborate dihydrate is a new borate. It was not known as a possible borate forming by hydrolysis of AB. Henceforth, it contributes to expanding the list of the possible borate by-products coming from AB.

In hydrolytic conditions, AB can be compared to NaBH<sub>4</sub>. The present work has shown that both encounter the same problems, namely difficult long-term storage of their aqueous alkaline solutions, safety issues due to uncontrolled H<sub>2</sub> generation, and precipitation of borates. In fact, AB in hydrolytic conditions encounters another problem. More than one borate seems to form, depending on the hydrolysis conditions. This is an issue from the recycling point of view. Further works are required to clear up this point, mainly because the industrial future of AB, if any, will be entirely dependent on its regeneration from its various borate by-products.

## Acknowledgments

UBD thanks the Agence Nationale pour la Recherche (ANR) for: (i) the LabEx CheMISyst project called A3 funded within the program “Investissement d’Avenir” with the reference ANR-10-LABX-05-01; (ii) the project called MobiDiC funded within the program “AAP Générique PRC” with the reference ANR-16-CE05-0009.

## References

- [1] Li H, Yang Q, Chen X, Shore SG. Ammonia borane, past as prolog. *J. Organomet. Chem.* 2014;751:60-6. <https://doi.org/10.1016/j.jorganchem.2013.08.044>
- [2] Gutowska A, Li L, Shin Y, Wang CM, Li XS, Linehan JC, Smith RS, et al. Nanoscaffold mediates hydrogen release and the reactivity of ammonia borane. *Angew Chem* 2005;117:3644-8. <https://doi.org/10.1002/anie.200462602>
- [3] Chandra M, Xu Q. A high-performance hydrogen generation system: Transition metal-catalyzed dissociation and hydrolysis of ammonia–borane. *J Power Sources* 2006;156:190-4. <https://doi.org/10.1016/j.jpowsour.2005.05.043>
- [4] Smythe NC, Gordon JC. Ammonia borane as a hydrogen carrier: Dehydrogenation and regeneration. *Eur J Inorg Chem* 2010;4:509-21. <https://doi.org/10.1002/ejic.200900932>
- [5] Demirci UB. Ammonia borane, a material with exceptional properties for chemical hydrogen storage. *Int J Hydrogen Energy* 2017;42:9978-10013. <https://doi.org/10.1016/j.ijhydene.2017.01.154>
- [6] Demirci UB. About the technological readiness of the H<sub>2</sub> generation by hydrolysis of B(–N)–H compounds. *Energy Technol* 2018;6:470-86. <https://doi.org/10.1002/ente.201700486>
- [7] Kojima Y, Suzuki K, Fukumoto K, Sasaki M, Yamamoto T, Kawai Y, Hayashi H. Hydrogen generation using sodium borohydride solution and metal catalyst coated on metal oxide. *Int J Hydrogen Energy* 2002;27:1029-34. [https://doi.org/10.1016/S0360-3199\(02\)00014-9](https://doi.org/10.1016/S0360-3199(02)00014-9)
- [8] Bartkus T, T'ien JS, Sung CJ. A semi-global reaction rate model based on experimental data for the self-hydrolysis kinetics of aqueous sodium borohydride. *Int J Hydrogen Energy* 2013;38:4024-33. <https://doi.org/10.1016/j.ijhydene.2013.01.041>
- [9] Chandra M, Xu Q. Dissociation and hydrolysis of ammonia-borane with solid acids and carbon dioxide: An efficient hydrogen generation system. *J Power Sources* 2006;159:855-60. <https://doi.org/10.1016/j.jpowsour.2005.12.033>
- [10] Jiang HL, Xu Q. Catalytic hydrolysis of ammonia borane for chemical hydrogen storage. *Catal Today* 2011;170:56-63. <https://doi.org/10.1016/j.cattod.2010.09.019>

- [11] Muir SS, Yao X. Progress in sodium borohydride as a hydrogen storage material: Development of hydrolysis catalysts and reaction systems. *Int J Hydrogen Energy* 2011;36:5983-997. <https://doi.org/10.1016/j.ijhydene.2011.02.032>
- [12] Akbayrak S, Özkar S. Ammonia borane as hydrogen storage materials. *Int J Hydrogen Energy* 2018;43:18592-606. <https://doi.org/10.1016/j.ijhydene.2018.02.190>
- [13] Alpaydın CY, Gülbay SK, Colpan CO. A review on the catalysts used for hydrogen production from ammonia borane. *Int J Hydrogen Energy* 2019; in press. <https://doi.org/10.1016/j.ijhydene.2019.02.181>
- [14] Andersson J, Grönkvist S. Large-scale storage of hydrogen. *Int J Hydrogen Energy* 2019;44:11901-19. <https://doi.org/10.1016/j.ijhydene.2019.03.063>
- [15] Kildahl NK. Bond energy data summarized. *J Chem Educ* 1995;72:423-424. <https://doi.org/10.1021/ed072p423>
- [16] Mohajeri N, T-Raissi A, Adebisi O. Hydrolytic cleavage of ammonia-borane complex for hydrogen production. *J Power Sources* 2007;167:482-8. <https://doi.org/10.1016/j.jpowsour.2007.02.059>
- [17] Liu CH, Wu YC, Chen BH, Hsueh CL, Ku JR, Tsau F. Hydrogen generated from hydrolysis of ammonia borane using cobalt and ruthenium based catalysts. *Int J Hydrogen Energy* 2012;37:2950-9. <https://doi.org/10.1016/j.ijhydene.2011.05.022>
- [18] Rachiero GP, Demirci UB, Miele P. Bimetallic RuCo and RuCu catalysts supported on  $\gamma$ -Al<sub>2</sub>O<sub>3</sub>. A comparative study of their activity in hydrolysis of ammonia-borane. *Int J Hydrogen Energy* 2011;36:7051-65. <https://doi.org/10.1016/j.ijhydene.2011.03.009>
- [19] Rachiero GP, Demirci UB, Miele P. Facile synthesis by polyol method of a ruthenium catalyst supported on  $\gamma$ -Al<sub>2</sub>O<sub>3</sub> for hydrolytic dehydrogenation of ammonia borane. *Catal Today* 2011;170:85-92. <https://doi.org/10.1016/j.cattod.2011.01.040>
- [20] Hannauer J, Demirci UB, Geantet C, Herrmann JM, Miele P. Enhanced hydrogen release by catalyzed hydrolysis of sodium borohydride-ammonia borane mixtures: a solution-state <sup>11</sup>B NMR study. *Phys Chem Chem Phys* 2011;13:3809-18. <https://doi.org/10.1039/C0CP02090G>
- [21] Ramachandran PV, Gagare PD. Preparation of ammonia borane in high yield and purity, methanolysis, and regeneration. *Inorg Chem* 2007;46:7810-7. <https://doi.org/10.1021/ic700772a>

- [22] Moussa G, Moury R, Demirci UB, Miele P. Borates in hydrolysis of ammonia borane. *Int J Hydrogen Energy* 2013;38:7888-95. <http://dx.doi.org/10.1016/j.ijhydene.2013.04.121>
- [23] Chou CC, Lee DJ, Chen BH. Hydrogen production from hydrolysis of ammonia borane with limited water supply. *Int J Hydrogen Energy* 2012;37:15681-15690. <https://doi.org/10.1016/j.ijhydene.2012.05.108>
- [24] Bowden M, Autrey T, Brown I, Ryan M. The thermal decomposition of ammonia borane: A potential hydrogen storage material. *Curr Appl Phys* 2008;8:498-500. <https://doi.org/10.1016/j.cap.2007.10.045>
- [25] Balakrishnan T, Bhagavannarayana G, Ramamurthi K. Growth, structural, optical, thermal and mechanical properties of ammonium pentaborate single crystal. *Spectrochim Acta* 2008;71:578-83. <https://doi.org/10.1016/j.saa.2008.01.026>
- [26] Salentine CG. High-field  $^{11}\text{B}$  NMR of alkali borates. Aqueous polyborate equilibria. *Inorg Chem* 1983;22:3920-4. <https://doi.org/10.1021/ic00168a019>
- [27] Jun L, Shuping X, Shiyang G. FT-IR and Raman spectroscopic study of hydrated borates. *Spectrochim Acta* 1995;51A:519-32. [https://doi.org/10.1016/0584-8539\(94\)00183-C](https://doi.org/10.1016/0584-8539(94)00183-C)
- [28] Applegarth LMSGGA, Pye CC, Cox JS, Tremaine PR. Raman spectroscopic and ab initio investigation of aqueous boric acid, borate, and polyborate speciation from 25 to 80°C. *Ind Eng Chem Res* 2017;56:13983-96. <https://doi.org/10.1021/acs.iecr.7b03316>
- [29] Peng J, Chen J, Dong Y, Li W. Investigations on Mg-borate kinetics and mechanisms during evaporation, dilution and crystallization by Raman spectroscopy. *Spectr Acta A: Mol Biomol Spectr* 2018;199:367-75. <https://doi.org/10.1016/j.saa.2018.03.063>
- [30] Kipcak A, Derun EM, Piskin S. Characterisation and determination of the neutron transmission properties of sodium–calcium and sodium borates from different regions in Turkey. *J Radioanal Nucl Chem* 2014;301:175-88. <https://doi.org/10.1007/s10967-014-3161-7>
- [31] NIST X-ray Photoelectron Spectroscopy Database. NIST Standard Reference Database 20, Version 4.1, <https://srdata.nist.gov/xps/Default.aspx>; 2012 [accessed November 2019].
- [32] Demir H, Şahin Ö, İzgi MS, Fıratoglu H. Production of granular boron oxide by calcination of ammonium tetraborate tetrahydrate. *Thermochim Acta* 2006;445:1-6. <https://doi.org/10.1016/j.tca.2006.03.019>

- [33] Gainsford GJ, Kemmitt T, Higham C. Redetermination of the borax structure from laboratory X-ray data at 145 K. *Acta Cryst.* 2008;E64:i24-5. <https://doi.org/10.1107/S1600536808010441>
- [34] Spessard JE. Investigations of borane equilibria in neutral salt solutions. *J Inorg Nucl Chem* 1970;32:2607-13. [https://doi.org/10.1016/0022-1902\(70\)80308-6](https://doi.org/10.1016/0022-1902(70)80308-6)
- [35] Mesmer RE, Baes CF, Sweeton. Acidity measurements at elevated temperatures. VI. Boric acid equilibria. *Inorg Chem* 1972;11:537-43. <https://doi.org/10.1021/ic50109a023>
- [36] Zhou YQ, Fang CH, Fang Y, Zhu FY, Cao LD. Polyborates in aqueous borate solution at 298.15 K. *Asian J Chem* 2012;24:29-32.
- [37] Brockman A, Zheng Y, Gore J. A study of catalytic hydrolysis of concentrated ammonia borane solutions. *Int J Hydrogen Energy* 2010;35:7350-6. <https://doi.org/10.1016/j.ijhydene.2010.04.172>
- [38] Uribe FA, Gottesfeld S, Zawodzinski Jr TA. Effect of ammonia as potential fuel impurity on proton exchange membrane fuel cell performance. *J Electrochem Soc* 2002;149:A293-6. <https://doi.org/10.1149/1.1447221>
- [39] Anastas P, Eghbali N. Green chemistry: principles and practice. *Chem Soc Rev* 2010;39:301-12. <https://doi.org/10.1039/B918763B>
- [40] Lapena-Rey N, Blanco JA, Ferreyra E, Lemus JL, Pereira S, Serrot E. A fuel cell powered unmanned aerial vehicle for low altitude surveillance missions. *Int J Hydrogen Energy* 2017;42:6926-40. <https://doi.org/10.1016/j.ijhydene.2017.01.137>
- [41] Liu CH, Chen BH. The concept about the regeneration of spent borohydrides and used catalysts from green electricity. *Materials* 2015;8:3456-66. <https://doi.org/10.3390/ma8063456>





+

